

Brain Gray Matter Changes in Migraine Patients With T2-Visible Lesions : A 3-T MRI Study

Maria A. Rocca, Antonia Ceccarelli, Andrea Falini, Bruno Colombo, Paola Tortorella, Luca Bernasconi, Giancarlo Comi, Giuseppe Scotti and Massimo Filippi

Stroke. 2006;37:1765-1770; originally published online May 25, 2006;

doi: 10.1161/01.STR.0000226589.00599.4d

Stroke is published by the American Heart Association, 7272 Greenville Avenue, Dallas, TX 75231

Copyright © 2006 American Heart Association, Inc. All rights reserved.

Print ISSN: 0039-2499. Online ISSN: 1524-4628

The online version of this article, along with updated information and services, is located on the World Wide Web at:

<http://stroke.ahajournals.org/content/37/7/1765>

Permissions: Requests for permissions to reproduce figures, tables, or portions of articles originally published in *Stroke* can be obtained via RightsLink, a service of the Copyright Clearance Center, not the Editorial Office. Once the online version of the published article for which permission is being requested is located, click Request Permissions in the middle column of the Web page under Services. Further information about this process is available in the [Permissions and Rights Question and Answer](#) document.

Reprints: Information about reprints can be found online at:
<http://www.lww.com/reprints>

Subscriptions: Information about subscribing to *Stroke* is online at:
<http://stroke.ahajournals.org/subscriptions/>

Brain Gray Matter Changes in Migraine Patients With T2-Visible Lesions

A 3-T MRI Study

Maria A. Rocca, MD; Antonia Ceccarelli, MD; Andrea Falini, MD; Bruno Colombo, MD; Paola Tortorella, MD; Luca Bernasconi, MD; Giancarlo Comi, MD; Giuseppe Scotti, MD; Massimo Filippi, MD

Background and Purpose—In migraine patients, functional imaging studies have shown changes in several brain gray matter (GM) regions. However, 1.5-T MRI has failed to detect any structural abnormality of these regions. We used a 3-T MRI scanner and voxel-based morphometry (VBM) to assess whether GM density abnormalities can be seen in patients with migraine with T2-visible abnormalities and to grade their extent.

Methods—In 16 migraine patients with T2-visible abnormalities and 15 matched controls, we acquired a T2-weighted and a high-resolution T1-weighted sequence. Lesion loads were measured on T2-weighted images. An optimized version of VBM analysis was used to assess regional differences in GM densities on T1-weighted scans of patients versus controls. Statistical parametric maps were thresholded at $P < 0.001$, uncorrected for multiple comparisons.

Results—Compared with controls, migraine patients had areas of reduced GM density, mainly located in the frontal and temporal lobes. Conversely, patients showed increased periaqueductal GM (PAG) density. Compared with patients without aura, migraine patients with aura had increased density of the PAG and of the dorsolateral pons. In migraine patients, reduced GM density was strongly related to age, disease duration, and T2-visible lesion load (r ranging from -0.84 to -0.73).

Conclusions—Structural GM abnormalities can be detected in migraine patients with brain T2-visible lesions using VBM and a high-field MRI scanner. Such GM changes comprise areas with reduced and increased density and are likely related to the pathological substrates associated with this disease. (*Stroke*. 2006;37:1765-1770.)

Key Words: magnetic resonance imaging ■ migraine

Positron emission tomography and MRI studies have shown functional abnormalities in the brain stem^{1,2} (in particular in the dorsal pons²) in migraine patients during an attack and in patients with chronic migraine,³ as well as an altered hypothalamic function in patients with cluster headache.⁴

It is plausible that such an altered function of brain structures might be associated to structural changes. Voxel-based morphometry (VBM) is a fully automated and unbiased method⁵ that is being increasingly used for the assessment of gray matter (GM) densities in several neurological conditions, including several pain conditions such as cluster headache,⁶ back pain,⁷ and migraine.⁸ Although these studies detected disease-specific GM abnormalities in patients with cluster headache⁶ and back pain,⁷ no GM abnormalities have been disclosed in migraine patients with and without aura.⁸ A variable that has not been considered in the latter study is the effect, if any, of the presence of macroscopic brain T2-visible lesions on GM changes in migraine patients. Brain T2-visible hyperintensi-

ties are a rather common finding in migraine patients.^{9,10} Data from a population-based cross-sectional MRI study have shown that female patients with migraine have a high risk of developing white matter (WM) hyperintense lesions, independently from the presence/absence of aura.¹¹ It is plausible that axons passing through these lesions might undergo retrograde degeneration with secondary GM changes.

The introduction of 3-T magnetic resonance systems in the clinical arena has improved the precision of the techniques for detecting central nervous system changes thanks to an increased signal-to-noise ratio and an increased spatial resolution.^{12,13} In this study, we applied VBM analysis to brain images acquired with a 3-T magnet to investigate whether changes in GM density are present in migraine patients with evidence of WM damage on conventional MRI compared with healthy controls. In case such changes were detected, additional analysis was preplanned in an attempt to provide some clues about their nature through the investigation of

Received January 2, 2006; final revision received March 27, 2006; accepted April 13, 2006.

From the Neuroimaging Research Unit (M.A.R., A.C., P.T., M.F.), CERMAC (M.A.R., A.F., G.S., M.F.), Department of Neuroradiology (A.F., G.S.), and Department of Neurology (B.C., L.B., G.C., M.F.), Scientific Institute and University Ospedale San Raffaele, Milan, Italy.

Correspondence to Dr Massimo Filippi, Neuroimaging Research Unit, Department of Neurology, Scientific Institute and University Ospedale San Raffaele, Via Olgettina, 60, 20132 Milan, Italy. E-mail massimo.filippi@hsr.it

© 2006 American Heart Association, Inc.

Stroke is available at <http://www.strokeaha.org>

DOI: 10.1161/01.STR.0000226589.00599.4d

their correlation with patients' demographic characteristics (age, disease duration), clinical manifestations of the disease (presence/absence of aura), and extent of macroscopic visible lesions.

Patients and Methods

We studied 16 migraine patients (7 with aura, 9 without aura; 15 women, 1 man; mean age 42.7 years, range 28 to 58 years; mean disease duration 24.8 years, range 2 to 48 years; mean number of attacks per year 20.3, range 12 to 244; mean time elapsed from the last attack 30 days, range 15 to 45 days)¹⁴ with ≥ 4 brain MRI hyperintense lesions on T2-weighted scans. The patients were recruited consecutively from the migraine population attending the outpatient clinics, Department of Neurology, Scientific Institute and University Ospedale San Raffaele, after having screened 57 patients. Patients with hypertension, hypercholesterolemia, diabetes mellitus, vascular/heart diseases, and other major systemic and neurological conditions were excluded. At the time MRI was performed, 5 patients were taking a prophylactic treatment for migraine. Fifteen healthy volunteers with no familial history of migraine, no previous history of neurological dysfunction (including migraine), and a normal neurological examination served as controls (13 women and 2 men; mean age 38.6 years, range 24 to 50 years [$P=0.2$ versus migraine patients]). All subjects were assessed clinically by a single neurologist who was unaware of the MRI results. Local ethical committee approval and written informed consent from all subjects were obtained before study initiation.

Using a 3-T Philips Intera scanner (Philips Medical Systems), the following scans of the brain were obtained: (1) T2-weighted turbo-spin echo images (repetition time [TR]/echo time [TE]=3000/120 ms; flip angle [FA]=90°, matrix size=512×512; field of view [FOV]=230 mm, 28, 4 mm thick, contiguous, axial slices), (2) fluid-attenuated inversion recovery sequence (TR/TE=11 000/120 ms; inversion time=2800 ms; FA=90°; matrix size=256×256; FOV=230 mm, 28, 4 mm thick, contiguous, axial slices), and (3) high-resolution 3D T1-weighted magnetization-prepared rapid acquisition gradient echo (MP-RAGE) sequence (TR/TE=25/4.6 ms; FA=30°; matrix size=256×256; FOV=230 mm, voxel size=1×1×1 mm³).

Lesions were identified on T2-weighted scans by consensus by 2 expert observers (M.A.R., A.F.) blinded to patient identity and marked on hardcopies. Fluid-attenuated inversion recovery scans were always used to increase confidence in lesion identification. Then, lesion volumes were measured on T2-weighted images using a local thresholding segmentation technique.¹⁰ VBM analysis was performed on 3D T1-weighted MP-RAGE images using statistical parametric mapping (SPM2) software.¹⁵ Before proceeding with VBM analysis, to avoid an erroneous classification of WM lesions as GM, T2-visible lesions were nulled out from the MP-RAGE scans. This procedure consisted in coregistration of the MP-RAGE images from each subject with the corresponding T2-weighted images using SPM2. Then, using MRIcro software, areas corresponding to T2-visible lesions were masked on the MP-RAGE images. The resulting MP-RAGE images were used for VBM analysis. Full details of the steps involved in the optimized method of VBM analysis have been described extensively previously.¹⁶ In short, this procedure involves extraction of the brain from the native skull space to determine ideal stereotactic normalization parameters. The native MRI scans are stereotactically normalized and segmented into GM, WM, and cerebrospinal fluid compartments. Then, a Jacobian modulation is applied to the data to preserve the absolute regional amount of GM from distortions introduced by the stereotactic normalization.⁵ The modulation step compensates for the warping effects of nonlinear normalization and preserves the variability in local tissue morphology. Finally, to improve the signal-to-noise ratio, the normalized images were smoothed with a 12-mm³ full width at half maximum Gaussian kernel. We used a customized GM template for spatial normalization, which was created using the MP-RAGE scans of both healthy controls and migraine patients. This procedure involved spatial normalization of the original images to the standard SPM T1

template, segmentation into WM and GM, averaging of the images and smoothing with an 8-mm full width at half maximum kernel.

Anatomical localization of the cerebral areas of altered GM density has been performed using the Talairach Daemon. A 3D anatomical atlas was also used to increase confidence in the definition of the anatomical locations of these areas.¹⁷

The comparison of GM maps between migraine patients and controls and between migraine patients with and without aura was performed on a voxel-by-voxel basis using SPM2 and a 2-sample *t* test. The GM densities were compared as absolute units. Decreases and increases of densities were investigated. The statistical parametric maps were thresholded at $P<0.001$, uncorrected for multiple comparisons at a voxel level. In brain stem areas where an a priori hypothesis was available, the cutoff value for significance was set at $P<0.05$, applying a small volume correction (SVC) for multiple comparisons by using a 12-mm radius.¹⁸ To assess the correlation of GM changes with clinical data (age and disease duration) and quantities derived from structural MRI (T2-lesion load), these metrics were entered into the SPM design matrix using basic models and linear regression analysis. To identify clusters of voxels of which GM density was related to these parameters, a threshold of $P<0.001$ uncorrected for multiple comparisons at a voxel level was used. Considering that age and disease duration are strongly inter-related, to define which of them had more influence on each these correlations, we performed a multivariate regression model including age and disease duration as independent variables using a stepwise selection procedure.

Results

All controls had normal brain MRI scans. In migraine patients, the mean number of T2-visible lesions was 26.9 (range 4 to 76; mean number of infratentorial lesions 0.1, range=0 to 3; mean number of periventricular lesions 7.7, range 1 to 34; mean number of iuxtacortical lesions 15.1, range 2 to 48; mean number of discrete lesions 2.75, range 1 to 10), the mean T2-weighted lesion load was 2.1 mL (range 0.02 to 11.2 mL). No statistically significant difference was found between patients with and without aura (mean T2-weighted lesion load: 1.5 mL, SD 2.1 mL in patients with aura versus 2.4 mL, SD 3.5 mL in patients without aura; $P=0.50$).

Compared with controls, migraine patients had several areas of reduced GM density, mainly located in the frontal and temporal lobes, bilaterally (Table 1; Figure 1). On the contrary, patients had an increased periacqueductal GM (PAG) density (SPM space coordinates: 4, -32, -22; peak *Z* score 3.43; $P<0.05$ after SVC; Figure 2).

The results obtained from the comparison of GM densities from the 2 groups of migraine patients (with and without aura) and controls are shown in Table 2. Compared with controls, migraine patients with aura also had an increased density of the PAG (SPM space coordinates: 0, -30, -22; peak *Z* score 4.17; $P<0.05$ after SVC) and the dorsolateral pons (SPM space coordinates: -3, -28, -21; peak *Z* score 3.40; $P<0.05$ after SVC). Compared with patients without aura, migraine patients with aura had decreased GM density of the right middle frontal gyrus (SPM space coordinates: 40, 28, 22; peak *Z* score 3.61; $P<0.001$ uncorrected) and increased density of the PAG (SPM space coordinates: -2, -30, -26; peak *Z* score 3.52; $P<0.05$ after SVC) and the dorsolateral pons (SPM space coordinates: -3, -29, -37; peak *Z* score 3.56; $P<0.05$ after SVC; Figure 3).

In Table 3, the correlation found between clinical (age, disease duration) and conventional MRI (T2 lesion load)

TABLE 1. Regions of Significantly Reduced GM Density in Migraine Patients Compared With Controls

Anatomical Regions	Brodmann Areas	SPM Space Coordinates x, y, z	Peak Z Scores
R SFG	6	25,12,54	4.98*
L SFG	10	-31, 64, 11	3.37
R Precentral gyrus	44	63, 13, 9	4.13*
L Precentral gyrus	44	-60, 11, 13	4.90*
R Anterior cingulated gyrus	32	1, 39, 25	3.91*
L Anterior cingulated gyrus	24	-2, 23, -2	3.95*
R MFG	10	41, 28, 32	4.23*
L MFG	10	-41, 28, 32	3.84
	10	-8, 52, -7	4.10*
	9	-25, 17, 53	3.72
R IFG	9	48, -2, 27	3.42
L IFG	...	-34, 49, 1	3.80
R STG	22	50, -49, 5	3.32
L STG	38	-47, 11, -11	3.58
R MTG	21	46, -9, -11	3.80
	39	56, -74, 22	4.29*
L MTG	21	-60, -7, -18	3.60
R ITG	37	55, -64, -18	3.66
L ITG	37	-43, -46, 27	3.70
	20	-56, -14, -34	4.44*
L Uncus	28	-18, -15, -38	4.61*

R indicates right; L, left; SFG, superior frontal gyrus; MFG, middle frontal gyrus; IFG, inferior frontal gyrus; STG, superior temporal gyrus; MTG, middle temporal gyrus; ITG, inferior temporal gyrus.

All the areas were significant at a $P < 0.001$, uncorrected for multiple comparisons at a voxel level. The asterisk identifies areas significant at $P < 0.05$, corrected for multiple comparisons (false discovery rate correction).

variables and regions of reduced GM density in migraine patients are shown. No correlation was found between the above-mentioned clinical and MRI variables and regions of increased GM density.

Discussion

Using VBM analysis on brain images obtained with a magnet operating at 3 T, we found that migraine patients with T2-visible hyperintense lesions have significant reductions of GM density of several brain regions when compared with healthy controls. Such changes were bilateral and mainly located in the cortex of frontal and temporal lobes and in the cingulum. In addition, such changes were similar between patients with and without aura, although there were some differences in the location of cortical areas, possibly because of the small number of subjects in each group. The role of the frontal lobe in pain processing has been underpinned by a recent morphological study,⁷ which has demonstrated in subjects with chronic back pain atrophy in the prefrontal cortex. Furthermore, functional imaging studies in migraine,^{1,2} cluster headache,^{6,19} and capsaicin-induced pain²⁰ have shown an association between pain and an abnormal activation of the cingulum and insula. At least 2 factors can explain decreased GM density in migraine patients. First, GM changes might be the consequence of

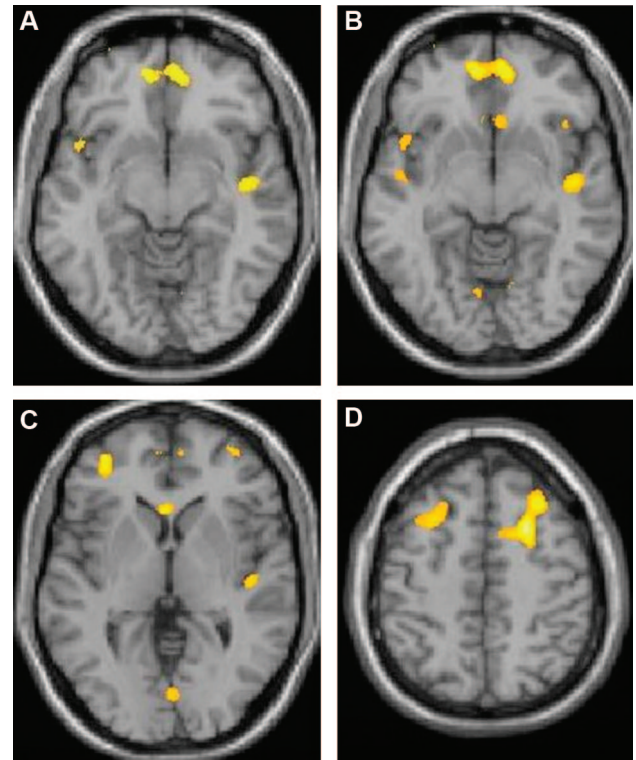


Figure 1. SPM regions superimposed on a high-resolution T1-weighted scan showing decreased GM density in migraine patients compared with controls ($P < 0.001$, uncorrected at a voxel level). Several areas are visible in the frontal and temporal lobes bilaterally (neurological convention).

repeated brain insults during the migraine attacks. During the past decades, several theories have been postulated to explain the genesis of the migraine attack. Recently, the vascular theory of Wolff²¹ has been confuted by accumulating evidence of mechanisms related to inflammation and excitotoxicity,²² prompting the formulation of the so-called “neurogenic inflammation” theory. Independently of the causative mechanism, the repetition of the attacks over time might result in a damage of selected cortical structures. This notion is strengthened by the correlation found in the present study between GM density reduction of some cortical regions and disease duration. The topographical distribution of GM changes observed in our patients might be

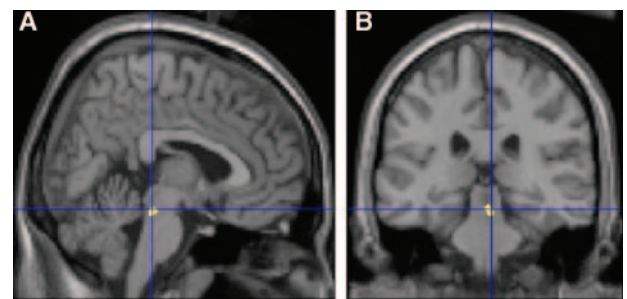


Figure 2. Sagittal (A) and coronal (B) views showing SPM regions superimposed on a high-resolution T1-weighted scan with increased GM density in migraine patients compared with healthy controls ($P < 0.001$, uncorrected at a voxel level; $P < 0.05$ after SVC). The PAG is visible in both sections (neurological convention).

TABLE 2. Regions of Significantly Reduced GM Density in Migraine Patients With and Without Aura Compared With Controls

Anatomical Regions	Brodmann Areas	Migraine Patients With Aura		Migraine Patients Without Aura	
		Coordinates x, y, z	Peak Z Scores	Coordinates x, y, z	Peak Z Scores
R SFG	6	27, 5, 55	5.05*
	9	24, 52, 37	3.50
R Precentral gyrus	6	61, -4, 32	3.52
L Precentral gyrus	44	-6, 23, -2	4.4*
L Anterior cingulated gyrus	24	-6, 23, -2	4.41*
R MFG	46	41, 29, 24	3.69
	10	39, 54, 12	3.41	38, 42, 22	5.61*
	9	2, 50, 33	4.90
L MFG	44	-61, 12, 12	4.18
	6	-26, 14, 51	3.39
	9	-42, 30, 32	4.74
	8	-23, 19, 53	3.68
R IFG	47	41, 20, -8	3.57
R STG	22	48, -18, 2	3.30
	38	42, 18, -33	3.43
L STG	38	-47, 13, 11	3.75
R MTG	21	43, -9, -12	3.58
L MTG	21	-48, -60, 9	3.75
L ITG	37	-49, -43, -22	4.17	-41, -47, -28	3.42
	20	-56, -16, -32	3.52
R Uncus	28	25, -17, -32	3.74

R indicates right; L, left; SFG, superior frontal gyrus; MFG, middle frontal gyrus; IFG, inferior frontal gyrus; STG, superior temporal gyrus; MTG, middle temporal gyrus; ITG, inferior temporal gyrus.

All the areas were significant at a $P < 0.001$, uncorrected for multiple comparisons at a voxel level. The asterisk identifies areas significant at a $P < 0.05$, corrected for multiple comparisons (false discovery rate correction).

explained by a different vulnerability of different cortical regions. Several cross-sectional and longitudinal studies of healthy individuals have indeed demonstrated that the frontal and the temporal cortices are particularly susceptible to age-related damage.^{16,23,24} Migraine-related changes might enhance such age-related susceptibility and result in an acceleration of the physiological brain shrinkage of particular GM areas. The

correlation that we found between patient age and cortical GM-reduced density supports this speculation. Second, an additional factor that might contribute to the observed GM changes is retrograde degeneration of axons passing through macroscopic

TABLE 3. Correlation Between Regions of Significantly Reduced GM Density in Migraine Patients and Clinical and MRI variables ($P < 0.001$, uncorrected for multiple comparisons at a voxel level)

Anatomical Region	Age	Disease Duration	T2 Lesion Load
R SFG	$r = -0.84$	* $r = -0.77$	$r = -0.71$
L SFG	* $r = -0.81$	$r = -0.77$...
R MFG	$r = -0.80$	* $r = -0.77$...
L MFG	* $r = -0.73$	$r = -0.81$	$r = -0.76$
R STG	* $r = -0.79$	$r = -0.75$	NS
R MTG	NS	$r = -0.79$	NS
L MTG	NS	$r = -0.78$	NS
L ITG	$r = -0.82$	NS	NS

R indicates right; L, left; SFG, superior frontal gyrus; MFG, middle frontal gyrus; IFG, inferior frontal gyrus; STG, superior temporal gyrus; MTG, middle temporal gyrus; ITG, inferior temporal gyrus.

The asterisk identifies which of these variables drives the correlation for each of the areas identified (see statistical analysis for details).

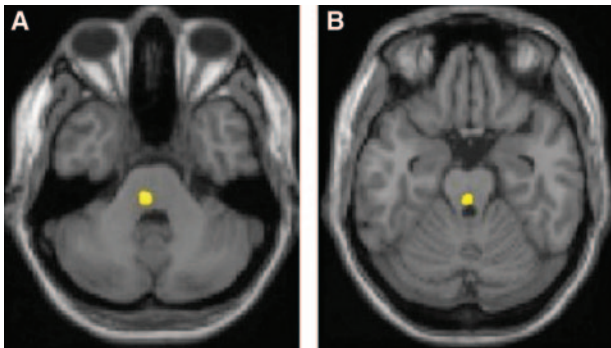


Figure 3. SPM regions superimposed on a high-resolution T1-weighted scan showing increased GM density in migraine patients with aura compared with those without aura ($P < 0.001$, uncorrected at a voxel level; $P < 0.05$ after SVC): A, Dorsolateral pons; B, PAG (neurological convention).

T2-visible lesions of the WM, as suggested by the correlation found between GM density and T2-visible lesion load.

Our results conflict with those of a previous VBM study⁸ in which no difference in GM density was found between migraine patients and controls. Because in both studies, patients were matched with appropriate control groups, this discrepancy might be attributable to the different radiological characteristics of the patients recruited. In our study, migraine patients were selected to have evidence of subcortical tissue damage on brain T2-weighted scans; this was because in the case of patients with normal MRI scans, it would have been impossible to know whether additional changes were actually not present or the technology used not sensitive enough. In addition, the higher field strength of the magnetic resonance magnet used in the present study (3 T versus 2 T) might also have resulted in an increased sensitivity for detecting subtle abnormalities and in a better segmentation of GM.

We also found an increased PAG density in migraine patients, which was more severe in migraine patients with aura. These latter patients also showed increased GM density in the dorsolateral pons. These findings fit with previous data showing an increased functional recruitment of brain stem regions of the dorsal pons² in a patient with migraine during an acute attack and with the results of 2 recent positron emission tomography studies showing an abnormal activation in the dorsolateral pons in a region that roughly corresponds to the one found in the present study during the migraine state in patients with and without aura.^{18,25} In addition, although abnormal functional activations have been detected in migraine patients without aura,^{1,2} several studies have also suggested a role of brain stem structures in the pathogenesis of migraine with aura. A case report showed functional MRI abnormalities in brain stem regions in a subject with migraine with aura.²⁶ These findings were subsequently confirmed in a cohort study.²⁷ In some of these patients, activation changes have also been detected in the dorsolateral pons and in the PAG. Finally, an abnormal iron homeostasis has been also documented in the PAG from migraine patients with and without aura,²⁸ possibly caused by repeated migraine attacks. All these results support the notion of PAG as a possible “generator” or “modulator” of the migraine attacks, possibly via a dysfunctional control of the trigeminovascular nociceptive system. It is indeed known that PAG stimulation modulates the activity of central trigeminal neurons that receive nociceptive input from dural and trigeminovascular afferents^{29,30} and that nonheadache patients can develop migraine-like episodes after stereotactic placement of electrodes in the PAG for treatment of other pain syndromes.³¹ Admittedly, we recruited a selected group of patients with migraine (ie, patients with WM hyperintense lesions) and, as a consequence, our results might not be generalized to the entire population of migraineurs. Therefore, we acknowledge the need to replicate these findings in a population of patients unselected for the presence of T2 brain abnormalities. In addition, considering the relatively small number of patients studied when considering patients with and without aura separately, the between-group comparison findings need to be replicated on larger samples of patients.

We believe that the increased GM density changes observed in our migraine patients are likely to be permanent and not related to transient increased function because all our patients were studied in a headache-free state. However, considering that definitive histopathological correlation in these patients are unlikely to ever be obtained, only a longitudinal MRI study of these patients would provide more definitive hints on this issue. At present, we can only speculate on the nature of the pathological changes underlying increased GM density in brain regions of migraine patients. First, a synaptic and neuritis size increase related to an experience-dependent plasticity can be advocated. The repetition of migraine attacks with the continuous activation of pain-related pathways might drive the formation of synapses, and these changes might lead to adaptive remodeling of neural circuits, as suggested for sensory experience³² and learning.³³ Second, increased GM density might be the consequence of neuronal loss and secondary reactive gliosis in those brain regions that experience significant functional changes during the migraine attacks. Finally, preapoptotic osmotic changes associated to early neuronal and glial pathology secondary to the vascular changes observed during the migraine attacks might also play a role in this context.

Disclosures

None.

References

- Weiller C, May A, Limmroth V, Juptner M, Kaube H, Schayck RV, Coenen HH, Diener HC. Brain stem activation in spontaneous human migraine attacks. *Nat Med*. 1995;1:658–660.
- Bahra A, Matharu MS, Buchel C, Frackowiak RS, Goadsby PJ. Brainstem activation specific to migraine headache. *Lancet*. 2001;357:1016–1017.
- Matharu MS, Bartsch T, Ward N, Frackowiak RS, Weiner R, Goadsby PJ. Central neuromodulation in chronic migraine patients with suboccipital stimulators: a PET study. *Brain*. 2004;127:220–230.
- May A, Bahra A, Buchel C, Frackowiak RS, Goadsby PJ. Hypothalamic activation in cluster headache attacks. *Lancet*. 1998;351:275–278.
- Ashburner J, Friston KJ. Voxel-based morphometry—the methods. *NeuroImage*. 2000;11:805–821.
- May A, Ashburner J, Buchel C, McGonigle DJ, Friston KJ, Frackowiak RS, Goadsby PJ. Correlation between structural and functional changes in brain in an idiopathic headache syndrome. *Nat Med*. 1999;5:836–838.
- Apkarian AV, Sosa Y, Sonty S, Levy RM, Harden RN, Parrish TB, Gitelman DR. Chronic back pain is associated with decreased prefrontal and thalamic grey matter density. *J Neurosci*. 2004;24:10410–10415.
- Matharu MS, Good CD, May A, Bahra A, Goadsby PJ. No change in the structure of the brain in migraine: a voxel-based morphometric study. *Eur J Neurol*. 2003;10:53–57.
- Fazekas F, Koch M, Schmidt R, Offenbacher H, Payer F, Freidl W, Lechner H. The prevalence of cerebral damage varies with migraine type: a MRI study. *Headache*. 1992;32:287–291.
- Rocca MA, Colombo B, Pratesi A, Comi G, Filippi M. A magnetization transfer imaging study of the brain in patients with migraine. *Neurology*. 2000;54:507–509.
- Kruit MC, van Buchem MA, Hofman PA, Bakkers JT, Terwindt GM, Ferrari MD, Launer LJ. Migraine as a risk factor for subclinical brain lesions. *J Am Med Assoc*. 2004;291:427–434.
- Barbier EL, Marrett S, Danek A, Vortmeyer A, van Gelderen P, Duyn J, Bandettini P, Grafman J, Koretsky AP. Imaging cortical anatomy by high-resolution MR at 3.0T: detection of the stripe of Gennari in visual area 17. *Magn Reson Med*. 2002;48:735–738.
- Schwint W, Kugel H, Bachmann R, Kloska S, Allkemper T, Maintz D, Pfliederer B, Tombach B, Heindel W. Magnetic resonance imaging protocols for examination of the neurocranium at 3 T. *Eur Radiol*. 2003;13:2170–2179.
- Headache Classification Committee of The International Headache Society. The International Classification of Headache Disorders, 2nd ed. *Cephalalgia*. 2004;24:1–160.

15. Friston KJ, Holmes AP, Worsley KP, Poline JB, Frith CD, Frackowiak RS. Statistical parametric maps in functional imaging: a general linear approach. *Hum Brain Mapp*. 1995;2:189–210.
16. Good CD, Johnsrude IS, Ashburner J, Henson RN, Friston KJ, Frackowiak RS. A voxel-based morphometric study of aging in 465 normal adult human brains. *NeuroImage*. 2001;14:21–36.
17. Duvernoy HM. *The Human Brain. Surface, Blood Supply, and Three-Dimensional Sectional Anatomy*. New York, NY: Springer Wien; 1999.
18. Afridi SK, Matharu MS, Lee L, Kaube H, Friston KJ, Frackowiak RS, Goadsby PJ. A PET study exploring the laterality of brainstem activation in migraine using glyceryl trinitrate. *Brain*. 2005;128:932–939.
19. May A, Goadsby PJ. Hypothalamic involvement and activation in cluster headache. *Curr Pain Headache Rep*. 2001;5:60–66.
20. May A, Kaube H, Buchel C, Eichten C, Rijntjes M, Juptner M, Weiller C, Diener HC. Experimental cranial pain elicited by capsaicin: a PET study. *Pain*. 1998;74:61–66.
21. Wolff HG. *Headache and Other Head Pain*. 2nd ed. New York, NY: Oxford University Press; 1963.
22. Waeber C, Moskowitz MA. Migraine as an inflammatory disorder. *Neurology*. 2005;64:S9–15.
23. Resnick SM, Goldszal AF, Davatzikos C, Golski S, Kraut MA, Metter EJ, Bryan RN, Zonderman AB. One-year age changes in MRI brain volumes in older adults. *Cereb Cortex*. 2000;10:464–472.
24. Salat DH, Buckner RL, Snyder AZ, Greve DN, Desikan RS, Busa E, Morris JC, Dale AM, Fischl B. Thinning of the cerebral cortex in aging. *Cereb Cortex*. 2004;14:721–730.
25. Afridi SK, Giffin NJ, Kaube H, Friston KJ, Ward NS, Frackowiak RS, Goadsby PJ. A positron emission tomographic study in spontaneous migraine. *Arch Neurol*. 2005;62:1270–1275.
26. Welch KM, Cao Y, Aurora S, Wiggins G, Vikingstad EM. MRI of the occipital cortex, red nucleus, and substantia nigra during visual aura of migraine. *Neurology*. 1998;51:1465–1469.
27. Cao Y, Aurora SK, Nagesh V, Patel SC, Welch KM. Functional MRI-BOLD of brainstem structures during visually triggered migraine. *Neurology*. 2002;59:72–78.
28. Welch KM, Nagesh V, Aurora SK, Gelman N. Periaqueductal grey matter dysfunction in migraine: cause or the burden of illness? *Headache*. 2001;41:629–637.
29. Bartsch T, Knight YE, Goadsby PJ. Activation of 5-HT(1B/1D) receptor in the periaqueductal grey inhibits nociception. *Ann Neurol*. 2004;56:371–381.
30. Knight YE, Bartsch T, Kaube H, Goadsby PJ. P/Q-type calcium-channel blockade in the periaqueductal grey facilitates trigeminal nociception: a functional genetic link for migraine? *J Neurosci*. 2002;22:RC213.
31. Veloso F, Kumar K, Toth C. Headache secondary to deep brain implantation. *Headache*. 1998;38:507–515.
32. Trachtenberg JT, Chen BE, Knott GW, Feng G, Sanes JR, Welker E, Svoboda K. Long-term in vivo imaging of experience-dependent synaptic plasticity in adult cortex. *Nature*. 2002;420:788–794.
33. Draganski B, Gaser C, Busch V, Schuierer G, Bogdahn U, May A. Neuroplasticity: changes in grey matter induced by training. *Nature*. 2004;427:311–332.